Archival Report

Biological Psychiatry

# Genetically Induced Retrograde Amnesia of Associative Memories After Neuroplastin Ablation

Soumee Bhattacharya, Rodrigo Herrera-Molina, Victor Sabanov, Tariq Ahmed, Emilia Iscru, Franziska Stöber, Karin Richter, Klaus-Dieter Fischer, Frank Angenstein, Jürgen Goldschmidt, Philip W. Beesley, Detlef Balschun, Karl-Heinz Smalla, Eckart D. Gundelfinger, and Dirk Montag

## ABSTRACT

**BACKGROUND:** Neuroplastin cell recognition molecules have been implicated in synaptic plasticity. Polymorphisms in the regulatory region of the human neuroplastin gene (*NPTN*) are correlated with cortical thickness and intellectual abilities in adolescents and in individuals with schizophrenia.

**METHODS:** We characterized behavioral and functional changes in inducible conditional neuroplastin-deficient mice.

**RESULTS:** We demonstrate that neuroplastins are required for associative learning in conditioning paradigms, e.g., two-way active avoidance and fear conditioning. Retrograde amnesia of learned associative memories is elicited by inducible neuron-specific ablation of *Nptn* gene expression in adult mice, which shows that neuroplastins are indispensable for the availability of previously acquired associative memories. Using single-photon emission computed tomography imaging in awake mice, we identified brain structures activated during memory recall. Constitutive neuroplastin deficiency or *Nptn* gene ablation in adult mice causes substantial electrophysiologic deficits such as reduced long-term potentiation. In addition, neuroplastin-deficient mice reveal profound physiologic and behavioral deficits, some of which are related to depression and schizophrenia, which illustrate neuroplastin's essential functions.

**CONCLUSIONS:** Neuroplastins are essential for learning and memory. Retrograde amnesia after an associative learning task can be induced by ablation of the neuroplastin gene. The inducible neuroplastin-deficient mouse model provides a new and unique means to analyze the molecular and cellular mechanisms underlying retrograde amnesia and memory.

***Keywords:*** Associative memory, Knockout mouse model, Learning impairment, Neuroplastin, Retrograde amnesia, Synaptic plasticity

http://dx.doi.org/10.1016/j.biopsych.2016.03.2107

Learning and memory, in particular associative memories, determine successful interaction with the environment. Memory loss (amnesia) characterizes dementias and other disorders of brain function, e.g., posttraumatic stress disorder. Learning and memory processes depend on synaptic architecture and plasticity. Cell adhesion molecules (CAMs) communicate extracellular and intracellular events, and neuronal CAMs such as neuroplastins, neurexins, neuroligins, neural CAM, and L1 are involved in synapse formation, modulation, and plasticity (1–4).

Neuroplastin isoforms (Np55 and Np65) are encoded by a single gene. Polymorphisms in the regulatory region of the human *NPTN* gene are correlated with cortical thickness and intellectual abilities in adolescents (5) and individuals with schizophrenia (6). Np55 shows widespread expression in various organs and cell types, whereas Np65 is brain-specific and restricted to neurons and undergoes *trans*-homophilic binding (1,7). Recombinant Np65- or Np65-specific antibodies can block long-term potentiation (LTP) in the hippocampal CA1 and CA3 (1). Furthermore, kainate induced seizures or induction of LTP increase Np65 in postsynaptic densities (1). Neuroplastins are binding partners of fibroblast growth factor receptors (8) and gamma-aminobutyric acid type A ($GABA_A$) receptors (9). Np65 interacts with the $GABA_A$ receptor $\alpha_2$ subunit and neuroplastin-deficient neurons exhibit impaired inhibitory transmission (9,10).

We generated inducible neuroplastin-deficient mice and analyzed the dependence of learning and memory and synaptic plasticity on neuroplastins. We show that neuroplastins are required for associative learning and memory, LTP expression, and hormonal homeostasis. Furthermore, inducible neuroplastin-deficient mice enabled us to elicit and investigate molecular mechanisms of retrograde amnesia.





ISSN: 0006-3223

## METHODS AND MATERIALS

### Statistical Analysis

Statview (SAS Institute, Inc., Cary, NC) and SPSS 19 (IBM Corp., Armonk, NY) were used for analysis of variance, post hoc analysis (Scheffé or Fisher's protected least significant difference), repeated-measures analysis of variance, and *t* tests. $p < .05$ was considered significant.

### Animals

Mice were kept with a 12-hour light/dark cycle and food and water ad libitum. All procedures were in accordance with institutional, state, and government regulations. For the generation of mutant mice see Supplemental Figures S1–S10, Supplemental Tables S1 and S2, and Supplemental Methods. $Nptn^{+/-}$ mice were backcrossed for more than 10 generations, and $Nptn^{lox/+}$ mice for more than five generations to C57BL/6-Crl. $Nptn^{lox/+}$ crossed with prion promoter CreERT mice (11) were maintained by inbreeding $Nptn^{lox/lox}$ and $Nptn^{lox/loxPr\text{-}CreERT}$ mice. CreERT was activated by daily intraperitoneal injection of 200 μL tamoxifen (10 mg/mL medical oil, T 5648; Sigma-Aldrich, St. Louis, MO) for 10 days.

### Antibodies

**Primary Antibodies.** Polyclonal antisera against immunoglobulin 1–3 and immunoglobulin 2–3 detecting Np65 and Np55 are described (1). Purchased antibodies were rat polyclonal homer (Acris Antibodies GmbH, Herford, Germany); rabbit polyclonal glucocorticoid receptor (Abcam, Cambridge, United Kingdom); mouse monoclonal glucocorticoid receptor; β-actin; glyceraldehyde 3-phosphate dehydrogenase (Santa Cruz Biotechnology, Inc., Heidelberg, Germany); goat polyclonal Np65 isoform-specific; sheep polyclonal neuroplastin-detecting Np65 and Np55 (R&D Systems, Minneapolis, MN); mouse monoclonal microtubule-associated protein 2; gephyrin; guinea pig polyclonal synapsin 1,2; vesicular GABA transporter; rabbit polyclonal synaptophysin 1 (Synaptic Systems GmbH, Göttingen, Germany); and mouse monoclonal pan-plasma membrane $Ca^{2+}$ adenosine triphosphatase (PMCA) clone 5F10 (Abcam).

**Secondary Antibodies.** Secondary antibodies were anti-mouse horseradish peroxidase (Dako Cytomation, Hamburg, Germany) and Cy5, anti-rabbit and anti-goat horseradish peroxidase and Cy5, anti-guinea pig Cy3 and Cy5, anti-sheep Cy3 (Jackson ImmunoResearch Laboratories, Inc., West Grove, PA), anti-goat Alexa Fluor 568, anti-rat and anti-mouse Alexa Fluor 488 (Molecular Probes Life Technologies Corporation, Grand Island, NY), and anti-rabbit Cy3 (Abcam).

### Protein Analysis

Dissected organs were homogenized and analyzed by sodium dodecyl sulfate polyacrylamide gel electrophoresis and western blotting as described elsewhere (12). Protein concentrations were determined by amido black assay. Representative western blots were reproduced more than five times with different animals and in different laboratories.

### Immunofluorescent Staining

Anaesthetized animals were perfused with phosphate-buffered saline (PBS) (pH 7.4) followed by 4% paraformaldehyde (10 mL/min, 10 minutes). Brains were postfixed in 4% paraformaldehyde (4°C overnight), serially incubated with 0.5 and 1 mol/L saccharose, frozen in methyl butane, and stored at –80°C. Free-floating cryostat sections (20 and 40 μm) from four or more animals per genotype were blocked with 5% bovine serum albumin or 20% horse serum in PBS, incubated with primary antibodies (0.3% Triton [Serva, Heidelberg, Germany], 10% horse serum in PBS, 36–48 hours, 4°C), washed, probed with secondary antibodies, washed, and mounted using Mowiol (Sigma-Aldrich, Taufkirchen, Germany) or Vectarshield (Vector Laboratories, Burlingame, CA) with 4′,6-diamidino-2-phenylindole. Stainings were reproduced in three or more sections per animal.

### Corticosterone Enzyme-Linked Immunosorbent Assay

Corticosterone concentrations were determined using an enzyme-linked immunosorbent assay kit (DEV9922; Demeditec Diagnostics, Kiel, Germany) according to the manufacturer's instructions.

### Behavior

Sex- and age-matched littermate $Nptn^{+/+}$ mice served as controls for $Nptn^{-/-}$ and $Nptn^{+/-}$ mice, and $Nptn^{lox/lox}$ mice as controls for $Nptn^{\Delta lox/loxPrCreERT}$ mice. The experimenter was not aware of the genotype. For initial characterization of $Nptn^{-/-}$ and $Nptn^{\Delta lox/loxPrCreERT}$ mice, the following tests were conducted sequentially during the light phase: neurologic examination, grip strength, rotarod, open field, O-maze, light/dark avoidance, water maze, shuttle box, and startle–prepulse inhibition, as described elsewhere (13–17). Grip strength was measured with a force sensor (TSE Systems GmbH, Bad Homburg, Germany). The latency to fall off the rotarod (TSE Systems GmbH) was determined in two training sessions (3-hour interval) with increasing speed (4–40 rpm, 5 minutes) and 4 days later at 16, 24, 32, and 40 rpm constant speed. Open-field (50 × 50-cm) exploration for 15 minutes was analyzed for path length, speed, and time spent in the center and corners and at the walls (VideoMot2 software; TSE Systems GmbH). Mice were placed in an O-maze (San Diego Instruments, San Diego, CA) for 5 minutes. Entries, time, speed, and distance in closed or open areas were analyzed (VideoMot2). For light/dark avoidance behavior, mice were placed in an illuminated compartment (250 lux, 25 × 25 cm) adjacent to a dark compartment (12.5 × 25 cm). Time spent within compartments and transitions between them were analyzed for 10 minutes. Reduced latencies entering the dark at a later exposure (on the last day of behavioral experiments) indicate long-term memory (15). Spatial learning was assessed in the hidden platform Morris water maze as described elsewhere (13) using VideoMot2 and Wintrack software (http://www.dpwolfer.ch/wintrack//index.html) (18). Associative learning was assessed by two-way active avoidance in a two-chambered shuttle-box (TSE Systems GmbH) with 10 seconds

of light as conditioning (CS) and electrical foot shock as unconditioned stimulus (5 seconds, 0.5 mA pulsed) delivered after the CS (80 trials/day, 5–15 seconds of stochastically varied intertrial intervals for 5 consecutive days). Compartment changes during CS were counted as conditioned avoidance reactions. The acoustic startle response to a stimulus (50 ms, 120 dB) and its inhibition by prepulses (PPI) (30 ms; 100 ms before startle stimulus with eight different intensities, 73–94 dB, 3-dB increments, 70 dB white noise background) was analyzed in a startle-box system (TSE Systems GmbH). Habituation (3 minutes) was followed by two startle trials and in pseudorandom order by 10 startle trials and five trials at each prepulse intensity with stochastically varied intertrial intervals (5–30 seconds). The maximal startle amplitude was measured by a sensor platform. Fear conditioning was conducted as described elsewhere (19) using distinct cohorts of mice. Mice were conditioned in an operant chamber (San Diego Instruments) by exploration (2 minutes) and auditory cue presentation (15 seconds), followed by a foot shock (2 seconds, 1.5 mA unpulsed) with one repetition. Twenty-four hours later, mice were placed in the training chamber (context, 5 minutes) and then returned to their home cage. One hour later, mice were placed in a novel environment (3 minutes) and then the auditory cue (CS) was presented (3 minutes). Freezing behavior (immobility) was recorded during all sessions. For memory tests after *Nptn* ablation, the procedure described for the second day was conducted again at 4 and 10 weeks after induction. Social interactions were analyzed by the three-chamber test as described elsewhere (20). Briefly, during three test phases (10 minutes each), the mouse could explore all compartments. In phase 1, the mouse was alone. In phase 2, an unfamiliar C57BL/6Crl mouse (same sex, stranger 1) was placed in one of the wire cups. In phase 3, another unfamiliar C57BL/6Crl mouse (same sex, stranger 2) was placed in the other cup. Time spent in each compartment, time in contact with strangers, and transitions between compartments were recorded. The tail suspension test was performed as described (21) with mice secured at the distal part of the tail. Duration of active struggling behavior (mobility time) was scored for 6 minutes, not considering passive limb or head movements or swinging motion as active struggling.

## Memory Assessment After Induced *Nptn* Ablation

Mice were trained in the water maze (5 consecutive days, 6 trails per day, hidden platform, fixed position), the light/dark avoidance paradigm, and the two-way active avoidance paradigm (80 trials per day until they reached ≥75% performance). Then mice were injected with tamoxifen for 10 days and were tested 8 weeks later in the water maze (two trials), light/dark avoidance, and shuttle box (80 trials). Mice analyzed by single-photon emission computed tomography (SPECT) or for relearning were subjected only to the two-way active avoidance paradigm.

## Electrophysiology in the CA1 Region of Hippocampal Slices

Preparation and methods applied were as detailed elsewhere (22). Briefly, the right hippocampus of 3- to 5-month-old mice (both sexes) killed by cervical dislocation was dissected out. Transverse slices (400 μm) prepared from the dorsal area were maintained at 32°C continuously perfused with artificial cerebrospinal fluid (ACSF) (2.2 mL/min, in mmol/L: NaCl, 124; KCl, 4.9; $NaH_2PO_4$, 1.2; $NaHCO_3$, 25.6; $CaCl_2$, 2; $MgSO_4$, 2; glucose, 10; saturated with 95% $O_2$ and 5% $CO_2$, pH 7.3–7.4). A tungsten electrode was placed in the CA1 stratum radiatum for stimulation. Evoked field excitatory postsynaptic potentials (fEPSPs) were recorded with a glass electrode (filled with ACSF, 3–7 MΩ). The descending slope of the fEPSP was used as a measure of this potential. Stimulation strength, adjusted eliciting a fEPSP slope of 35% of the maximum (determined by input–output curves), was kept constant. Paired-pulse facilitation was investigated applying two pulses in rapid succession (interpulse intervals of 10, 20, 50, 100, 200, and 500 ms, respectively) at 120-second intervals. During baseline recording, three single stimuli (0.1-ms pulse width; 10-second intervals) were measured every 5 minutes and averaged. To induce strong LTP, theta-burst stimulation (10 bursts of four stimuli at 100 Hz, applied every 200 ms; pulse width of 0.2 ms) was repeated three times every 10 minutes, with evoked responses at 1, 4, and 7 minutes during the three conditioning protocols. Thereafter, responses were recorded every 5 minutes for 2 hours.

Postsynaptic currents from single CA1 pyramidal cells were recorded in transverse vibratome slices (400 μm, Microm HM650V; Thermo Scientific, Waltham, MA) from the medial hippocampus placed for 90 minutes in an incubation chamber containing ACSF and continuously perfused (95% $O_2$/5% $CO_2$, room temperature). Whole-cell voltage clamp recordings were performed at 32°C (MultiClamp 700B patch-clamp amplifier; Molecular Devices, Sunnyvale, CA). Data were collected with pClamp software (Axon Instruments, Union City, CA). Borosilicate glass recording electrodes were filled with the following solution (in mmol/L): 135 $CsMeSO_4$, 4 NaCl, 4 Mg–adenosine triphosphate, 0.5 ethylene glycol bis-2-aminoethyl ether-N,N′,N″,n′-tetraacetic acid-Na, 0,3 Na–guanosine triphosphate, 10 K–4-(2-hydroxyethyl)-1-piperazineethanesulfonic acid, 5 QX-314; pH 7.3 (pipette resistance, 3–5 MΩ). Access resistance was 10–20 MΩ and then compensated to 75%. If input resistance changed more than 25%, the neuron was excluded.

Based on reversal potential, miniature excitatory postsynaptic currents (mEPSCs) and miniature inhibitory postsynaptic currents (mIPSCs) were mostly measured consecutively from the same neurons (23–25). First, mEPSCs were recorded at the reversal potential for $GABA_A$ receptor-mediated events (−60 mV); then mIPSCs were recorded at the reversal potential for glutamatergic currents (+10 mV) with tetrodotoxin (1 μmol/L) present. Blocking mEPSCs by 20 μmol/L 6-cyano-7-nitroquinoxaline-2,3-dione and 10 μmol/L d-aminophosphonovalerate verified their glutamatergic nature. The mIPSCs were blocked by 100 μmol/L picrotoxin. Data were low-pass filtered at 2 kHz and acquired at 10 kHz using Digidata 1440 and pClamp 10 software (Molecular Devices). The mEPSCs and mIPSCs offline analysis used MiniAnalysis software (version 6.0.7; Synaptosoft, Decatur, GA).

## SPECT Imaging

We used SPECT imaging of regional cerebral blood flow for in vivo mapping of spatial patterns of neuronal activity in the brains of awake behaving mice (26). Catheters were placed into

the right external jugular veins 2 days before experiments (26). In the shuttle box, mice were injected during habituation (3 minutes) with saline, followed by $^{99m}$Tc-hexmethylpropyleneamineoxime ($^{99m}$Tc-HMPAO) (250 μL, 25 μL/min) during the initial 10 minutes of the paradigm consisting of 80 trials. The average injected dose was 67.5 MBq of $^{99m}$Tc at 250 μL per animal. After the shuttle box experiment, animals were anesthetized and scanned with a four-head NanoSPECT/CT scanner (Mediso, Hungary) as described elsewhere (26). The SPECT images were reconstructed at an isotropic voxel size of 338 μm using the manufacturer's software (HiSPECT; SCIVIS, Göttingen, Germany) and aligned with a high-resolution magnetic resonance mouse brain data set (27,28) (MPI-Tool 6.36; Advanced Tomo Vision, Kerpen, Germany). The SPECT brain data were cut out of the SPECT data in Osirix (64-bit, version 5.7.1; Pixmeo SARL, Bernex, Switzerland) using a whole-brain volume of interest made from the template by Ma and colleagues (27,28). Brain SPECT data were global mean normalized using MPI-Tool software. In the voxelwise analysis, unpaired *t* tests were made to compare brain tracer distribution in *Nptn*$^{\Delta lox/loxPrCreERT}$ ($n = 7$)

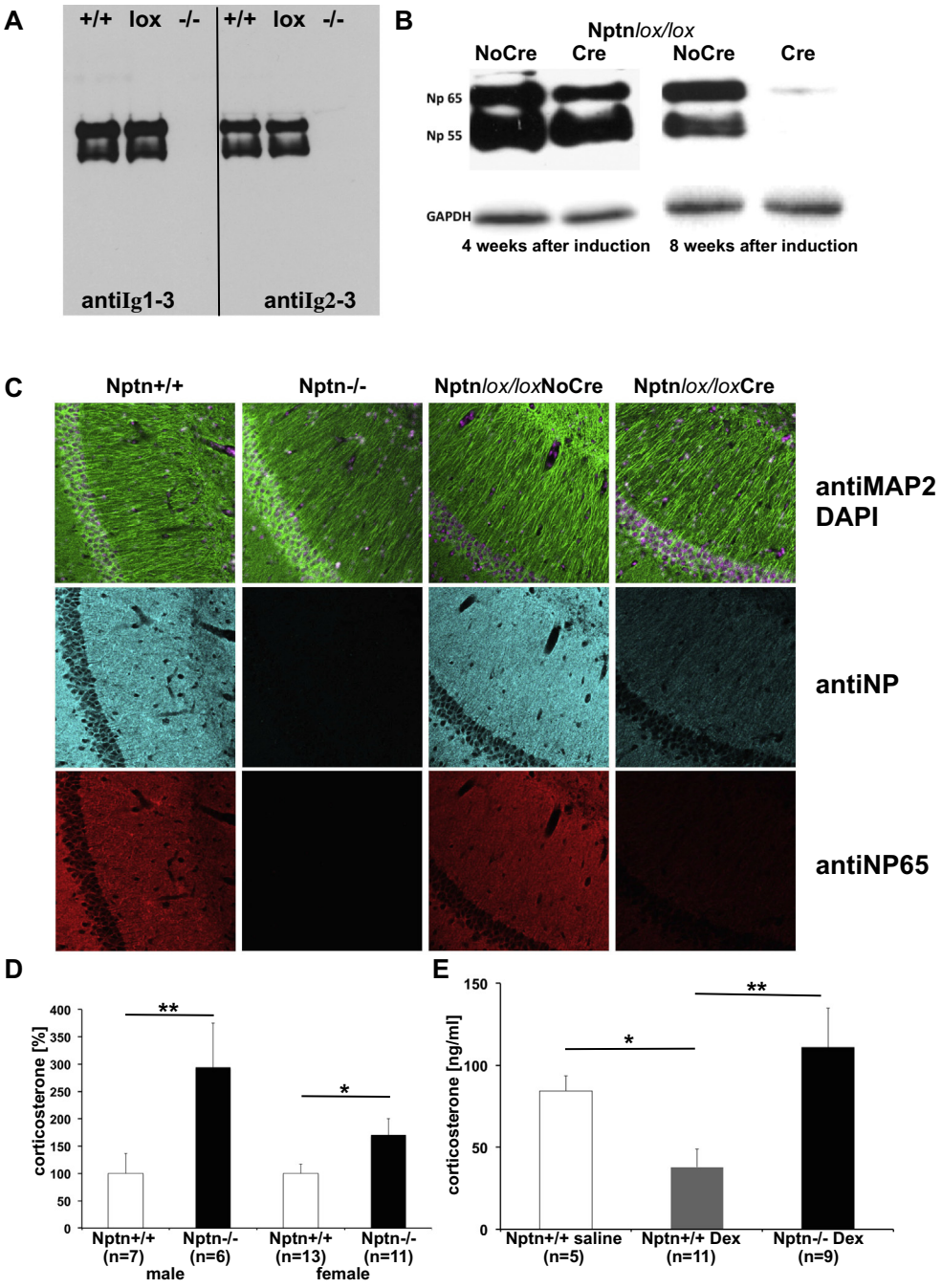


**Figure 1.** Characterization of *Nptn*$^{-/-}$ mice and impaired corticosterone regulation. **(A)** Western blot of membrane fractions (20 μg protein per lane) from brains of wild-type (*Nptn*$^{+/+}$), *Nptn*$^{lox/lox}$ (*lox*), and *Nptn*$^{-/-}$ mice. Polyclonal antibodies against immunoglobulin domains 1–3 (left) or 2–3 (right) of neuroplastin detecting the Np65 and Np55 isoforms were used. **(B)** Western blot of membrane fractions (20 μg protein per lane) from brains of *Nptn*$^{\Delta lox/loxPrCreERT}$ (Cre) or control *Nptn*$^{lox/lox}$ mice (NoCre) 4 and 8 weeks after induction by tamoxifen probed with antibodies against immunoglobulin domains 2–3 of neuroplastin and glyceraldehyde 3-phosphate dehydrogenase (GAPDH) as loading control. **(C)** Immunohistochemistry for anti-microtubule-associated protein 2 (antiMAP2) (green) and 4′,6-diamidino-2-phenylindole (DAPI) (magenta) (top row), anti-neuroplastins (antiNP) (cyan) (middle row), or anti-neuroplastin 65 isoform (antiNP65) (red) (bottom row) in the hippocampus of wild-type (*Nptn*$^{+/+}$), *Nptn*$^{-/-}$, and *Nptn*$^{\Delta lox/loxPrCreERT}$ (Nptn*lox/lox*Cre) or control *Nptn*$^{lox/lox}$ mice (Nptn*lox/lox*NoCre) 8 weeks after induction by tamoxifen. **(D)** Elevated morning serum corticosterone levels in neuroplastin-deficient mice (*Nptn*$^{-/-}$) compared with wild-type (*Nptn*$^{+/+}$) analyzed by enzyme-linked immunosorbent assay. **(E)** After a dexamethasone challenge (Dex), serum corticosterone levels are higher in male neuroplastin-deficient (*Nptn*$^{-/-}$) mice. All data are presented as means ± SEM; all *p* values are derived from Scheffé post hoc test after one-way analysis of variance (*$p < .05$; **$p < .01$; ***$p < .001$).

versus $Nptn^{lox/lox}$ control mice ($n$ = 9) using MagnAn software (version 2.4; BioCom, Uttenreuth, Germany). Following common procedures in small-animal radionuclide imaging (29–31), uncorrected $p$ values were used. Results were illustrated using Osirix and Photoshop (version CS4; Adobe Systems Software, San Jose, CA).

## RESULTS

Lox sites were introduced into the *Nptn* gene ($Nptn^{tmloxexon1lox}$ [$Nptn^{lox}$]), allowing Cre-recombinase–mediated permanent or inducible deletion of exon 1 encoding the start codon and the signal sequence (Supplemental Figure S1). Constitutively neuroplastin-deficient mice ($Nptn^{-/-}$) were generated by intercrossing heterozygous mice ($Nptn^{+/-}$) obtained after germ line excision of exon 1 ($Nptn^{tm\Delta exon1}$) by a constitutively expressed Cre-recombinase (32). In $Nptn^{-/-}$ mice, neuroplastins were undetectable in the brain and other organs (Figure 1A, C, Supplemental Table S1). $Nptn^{-/-}$ mice had a reduced life span (Supplemental Figure S2), body size, and weight, and male-specific incompetency to sire offspring (not shown). The gross brain architecture was not affected and magnetic resonance imaging morphometry showed normal anatomy of $Nptn^{-/-}$ brains with no significant size abnormalities (Supplemental Table S2, Supplemental Figure S3). Several endocrinologic factors, e.g., blood glucose levels, insulin regulation, and

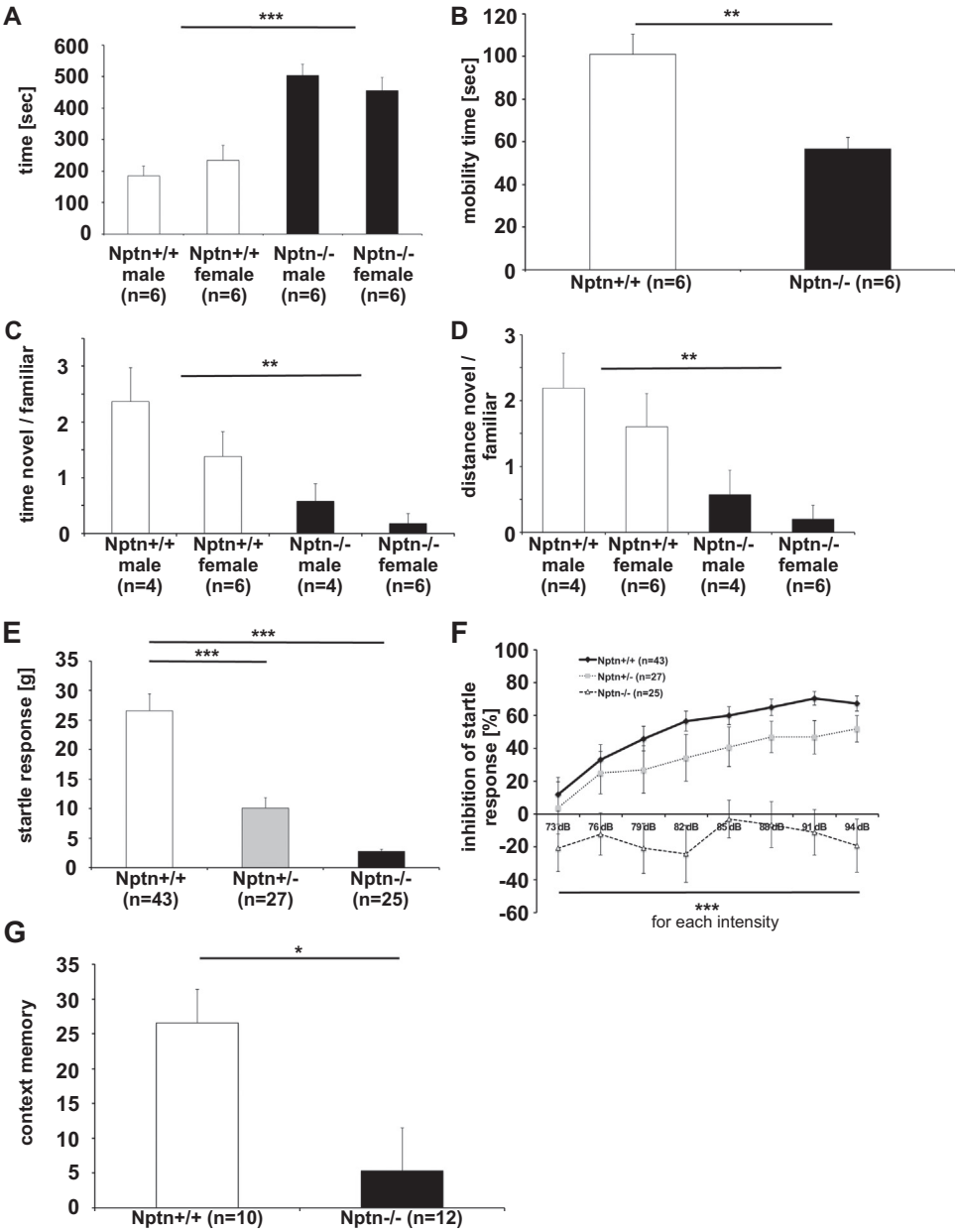


**Figure 2.** Behavioral deficits in $Nptn^{-/-}$ mice. **(A)** Increased preference for the center of an open field by $Nptn^{-/-}$ mice compared with wild-type ($Nptn^{+/+}$) mice. **(B)** Reduced active mobility time during the tail suspension test of male $Nptn^{-/-}$ mice. **(C, D)** Impaired social interaction of $Nptn^{-/-}$ mice in three-chamber assays. **(C)** Social novelty recognition (interaction with novel wild-type mouse of the same sex vs. familiarized wild-type mouse of the same sex). **(D)** Activity in the compartment of the strange mouse. **(E)** Reduced magnitude of the startle response of heterozygous ($Nptn^{+/-}$) and $Nptn^{-/-}$ mice. **(F)** Inhibition of the startle response by prepulses (PPI) with the given intensity as percentage of the startle response for $Nptn^{+/+}$, $Nptn^{+/-}$, and $Nptn^{-/-}$ mice (one-way ANOVA for all prepulse intensities: $p < .001$). **(G)** Reduced context memory (% freezing time shock minus neutral context) after fear conditioning in $Nptn^{-/-}$ mice. All data are presented as means ± SEM; all $p$ values are derived from Scheffé post hoc test after one- or two-way analysis of variance (*$p < .05$; **$p < .01$; ***$p < .001$).

thyroid (T3 and T4) and growth hormone levels were normal (Supplemental Figure S4). However, *Nptn*$^{-/-}$ mice had altered hypothalamic-pituitary-adrenal (HPA) axis correlates, namely elevated corticosterone levels, both basal and after a dexamethasone suppression test (Figure 1D, E) and decreased corticotropin-releasing hormone messenger RNA and glucocorticoid receptor levels in brain (Supplemental Figure S4).

Depression is associated with high cortisol levels, the analog of mouse corticosterone, and HPA axis dysregulation (33). Therefore, we tested *Nptn*$^{-/-}$ mice for core features of depression-related behavior including stress resilience, anxiety, social interaction, motivation, and despair. *Nptn*$^{-/-}$ mice displayed less anxious behavior in open-field (Figure 2A, Table 1) and light/dark avoidance tests (Supplemental Figure S5D) and higher preference for a familiarized over an unfamiliar mouse, which indicated altered social interactions (Figure 2C, D). Although male *Nptn*$^{-/-}$ mice did not exhibit consummatory anhedonia in the sucrose preference test (not shown), lack of motivation in the alternating T maze (not shown) and higher immobility in the tail suspension test indicated depressive-like behavior (Figure 2B).

While fundamental functions of the nervous system, e.g., reflexes and sensory abilities, appeared normal, neurologic deficits were apparent in specific tests including reduced motoric capabilities (grip strength and rotarod) (Supplemental Figure S5C, D) and aberrant swimming behavior (diving) in the Morris water maze. Furthermore, sensorimotor gating as examined by the startle response and its PPI (Figure 2E, F), associative learning as analyzed by fear conditioning (Figure 2G), and active avoidance learning (Figure 3A) revealed evident cognitive deficits in *Nptn*$^{-/-}$ mice.

These cognitive deficits suggested important roles of neuroplastins in learning and memory. To differentiate developmental from mature neuronal functions, we ablated neuronal neuroplastin expression in adult *Nptn*$^{lox/lox}$ mice by activating prion promoter-driven CreERT recombinase (11) with tamoxifen (*Nptn*$^{\Delta lox/loxPrCreERT}$). Immunoblot analysis showed about 65% reduced neuroplastin levels in the brain 4 weeks after induction, which further decreased to just detectable levels after 2 months (Figure 1B). When the behavior of *Nptn*$^{\Delta lox/loxPrCreERT}$ mice was analyzed more than 4 weeks after induction, their performance was similar to that of control mice without Cre with respect to grip strength, social interaction, motor abilities, and startle response (Supplemental Figure S6, Table 1). However, PPI of the startle response was slightly affected (Supplemental Figure S6E). Significantly reduced startle response and PPI in heterozygous *Nptn*$^{+/-}$ mice (Figure 2E, F) indicated that 50% of less of neuroplastin expression, either throughout life or after ablation in adulthood, affects PPI, a candidate endophenotype of schizophrenia.

Strikingly, associative learning in the shuttle box was abolished in induced *Nptn*$^{\Delta lox/loxPrCreERT}$ mice (Figure 3B). Investigating information acquisition, retention, access, and retrieval of memories, we first trained *Nptn*$^{lox/loxPrCreERT}$ mice in the shuttle box to high performance (greater than 75% correct responses) before inducing gene ablation. Two months after induction (Figure 3C), tamoxifen-treated control mice (*Nptn*$^{lox/lox}$ without Cre-recombinase) retained more than 50% of their previous performance, whereas *Nptn*$^{\Delta lox/loxPrCreERT}$ mice induced after training performed as poorly as did naive mice, displaying complete retrograde amnesia. Like naive induced *Nptn*$^{\Delta lox/loxPrCreERT}$ mice, the amnestic mice could not relearn the association even after extensive training (Figure 3D). These results demonstrate that neuroplastins are essential for learning and retention, and/or the retrieval of associative memories. Similar results were obtained using white noise instead of light as the conditioning stimulus (not shown), which showed stimulus modality independence of the retrograde amnesia. Furthermore, *Nptn*$^{-/-}$ mice displayed deficits in the context memory after fear conditioning (Figure 2G), which suggests that associative learning and memory are impaired task-independently. In agreement with these findings, *Nptn*$^{lox/loxPrCreERT}$

**Table 1. Behavior of *Nptn*$^{-/-}$ and *Nptn*$^{\Delta lox/loxPrCreERT}$ Mice**

| Test | *Nptn*$^{-/-}$ | *Nptn*$^{\Delta lox/loxPrCreERT}$ Ablation Before Tests | *Nptn*$^{\Delta lox/loxPrCreERT}$ Ablation After Training |
|---|---|---|---|
| Grip Strength | *Nptn*$^{-/-}$ reduced (Supplemental Figure S5A) | Not different (Supplemental Figure S6A) | |
| Rotarod | *Nptn*$^{-/-}$ reduced (Supplemental Figure S5B) | *Nptn*$^{\Delta lox/loxPrCreERT}$ slightly improved (Supplemental Figure S6B) | |
| Open Field | *Nptn*$^{-/-}$ more in center (Figure 2A) | Not different (not shown) | |
| O Maze | Not different (Supplemental Figure S5C) | Not different (not shown) | |
| Light/Dark Avoidance | *Nptn*$^{-/-}$ more transitions, more time in light (Supplemental Figure S5D) | Not different (not shown) | |
| Light/Dark Avoidance Memory | Not different (Supplemental Figure S5D) | Not different (not shown) | Not different (Supplemental Figure S7C) |
| Shuttle Box Two-Way Active Avoidance | *Nptn*$^{-/-}$, do not acquire task (Figure 3A) | *Nptn*$^{\Delta lox/loxPrCreERT}$, do not acquire task (Figure 3B) | *Nptn*$^{\Delta lox/loxPrCreERT}$, retrograde amnesia (Figure 3C, D) |
| Startle Response and Prepulse Inhibition (PPI) | *Nptn*$^{-/-}$ reduced startle response, reduced PPI (Figure 2E, F) | Startle not different, *Nptn*$^{\Delta lox/loxPrCreERT}$, slightly reduced PPI (Supplemental Figure S6D, E) | |
| Fear Conditioning | *Nptn*$^{-/-}$ reduced context memory (Figure 2G) | | *Nptn*$^{\Delta lox/loxPrCreERT}$ reduced context memory (Figure 3E, F) |
| Social Interaction | *Nptn*$^{-/-}$ less time, novel/familiar, and distance (Figure 2C, D) | Not different (Supplemental Figure S6C) | |
| Tail Suspension | *Nptn*$^{-/-}$ less active mobility (Figure 2B) | | |

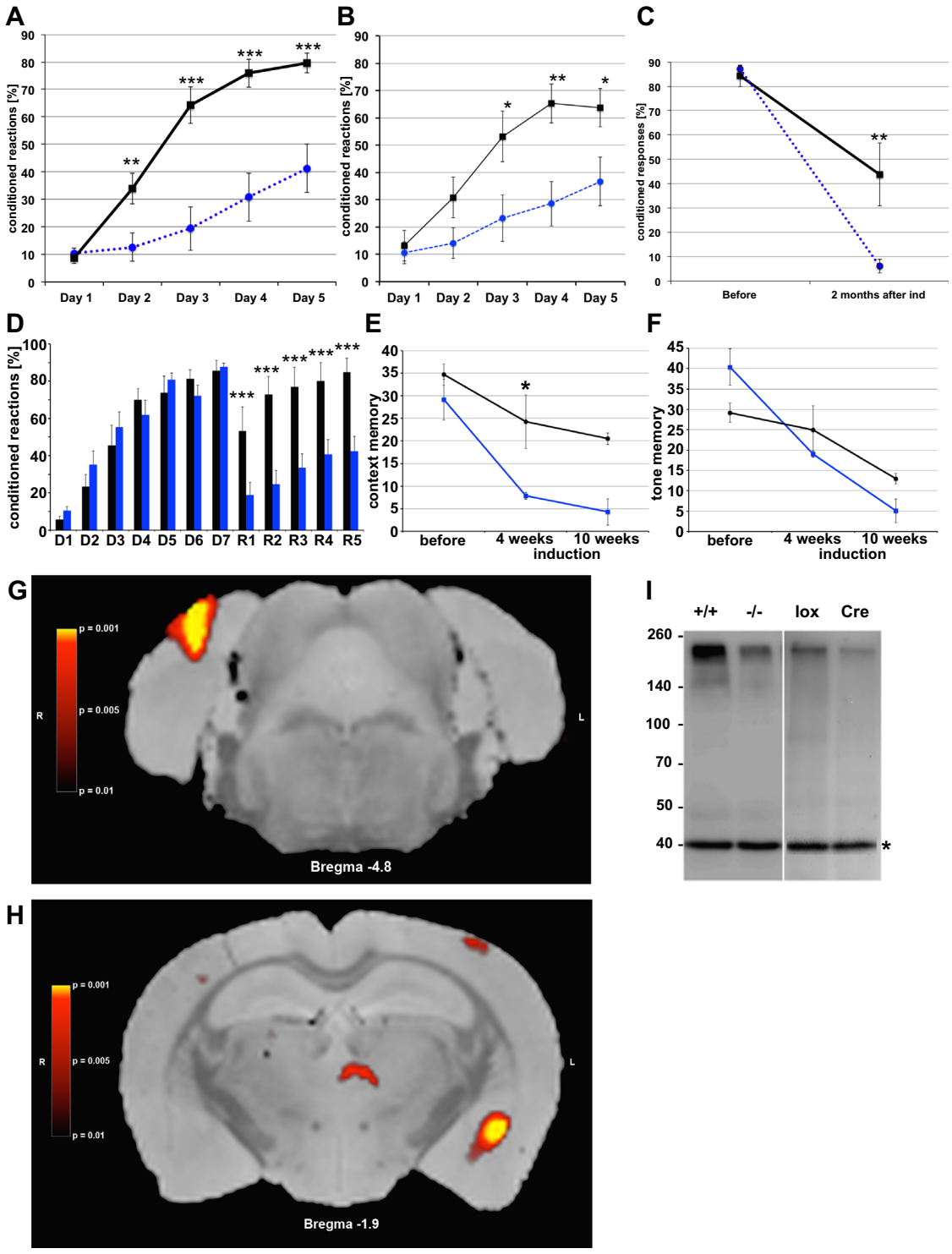
A
conditioned reactions [%]
Day 1
Day 2
Day 3
Day 4
Day 5
B
conditioned reactions [%]
C
conditioned responses [%]
Before
2 months after ind
D
conditioned reactions [%]
D1 D2 D3 D4 D5 D6 D7 R1 R2 R3 R4 R5
E
context memory
before
4 weeks
10 weeks
induction
F
tone memory
G
p = 0.001
p = 0.005
p = 0.01
R
L
Bregma -4.8
H
Bregma -1.9
I
+/+
-/-
lox
Cre
260
140
100
70
50
40

mice that are conditioned to fear before induction displayed significantly less context memory 4 weeks after induction (Figure 3E) but similar tone memory (Figure 3F) compared with control mice. The same *Nptn*$^{lox/loxPrCreERT}$ animals trained in the shuttle box had been trained in water maze and light/dark-avoidance paradigms before induction. Interestingly, neuroplastin ablation did not affect water maze performance or memory for the dark compartment (Supplemental Figure S7), which demonstrated the specificity of retrograde amnesia for associative memories. Loss of memory retrieval capabilities might be associated with alterations in activity patterns of relevant brain regions. Therefore, we traced regional cerebral blood flow during memory recall in the shuttle box by $^{99m}$Tc-HMPAO infusion and analyzed it by SPECT (26). Trained to 75% or greater correct responses before induction, at 8 weeks after induction *Nptn*$^{\Delta lox/loxPrCreERT}$ and *Nptn*$^{lox/lox}$ mice showed different activation patterns in the shuttle box (Figure 3G, H). As a key finding, $^{99m}$Tc uptake in the right primary visual cortex of induced *Nptn*$^{\Delta lox/loxPrCreERT}$ mice, compared with *Nptn*$^{lox/lox}$ control mice, was significantly increased ($p < .001$). This difference argues for an increased workload in processing of the visual stimulus in the induced *Nptn*$^{\Delta lox/loxPrCreERT}$ mice and might reflect an increase in task difficulty for these mice and/or differences in familiarity with the stimulus.

In *Nptn*$^{-/-}$ mice, we previously observed about 30% less excitatory synapses in the hippocampal CA1 region and the dentate gyrus, areas with highest Np65 levels in wild-type mice, whereas in CA3, which normally expresses less Np65, the number of synapses was unaltered (10). Ultrastructurally, no obvious abnormalities of synapses are observed in the hippocampal CA1 region of *Nptn*$^{-/-}$ mice (Supplemental Figures S8 and S9). Furthermore, the number of GABAergic synapses is not affected by constitutive loss of neuroplastins (Supplemental Figure S10). Therefore, part of the complex phenotype of *Nptn*$^{-/-}$ mice may result from disbalance of excitatory glutamatergic and inhibitory GABAergic synapses. Two months after inducible ablation of neuroplastin expression in adult *Nptn*$^{\Delta lox/loxPrCreERT}$ mice, we observed a slight increase in inhibitory CA1 synapses but no loss or disassembly of excitatory synapses after establishment of neuronal connectivity (Supplemental Figure S10).

Interestingly, we detected significantly reduced amounts of PMCAs in both *Nptn*$^{-/-}$ and *Nptn*$^{\Delta lox/loxPrCreERT}$ mice (Figure 3I). Because PMCAs restore normal $Ca^{2+}$ levels after neuronal activation (34), fewer PMCAs may result in altered $Ca^{2+}$ homeostasis and distribution in intracellular stores. Indeed, extrusion of calcium is an effective regulator of synaptic plasticity in neurons (35).

In the hippocampus of *Nptn*$^{-/-}$ mice, basal synaptic transmission evaluated by fEPSPs was normal (Figure 4A). Analysis of short-term plasticity revealed significantly increased paired-pulse facilitation in *Nptn*$^{-/-}$ synapses at longer interpulse intervals between 50 and 500 ms (Figure 4B). In agreement with a reduced excitatory–inhibitory ratio resulting from fewer glutamatergic synapses, LTP was impaired in *Nptn*$^{-/-}$ mice (Figure 4C) and mEPSC amplitudes were reduced (Figure 4D). The mEPSC frequencies showed a similar reduction; however, they did not reach the level of significance owing to a higher variance. No differences were found in mIPSCs (Figure 4E).

To differentiate developmental from mature neuroplastin functions, we measured the same parameters after *Nptn* ablation in adult *Nptn*$^{\Delta lox/loxPrCreERT}$ mice (Figure 4F–J). Basal synaptic transmission was normal (Figure 4F), but short-term plasticity was significantly reduced at short interpulse intervals between 10 and 50 ms (Figure 4G), which indicated affected GABAergic inhibition and presynaptic functions. As for *Nptn*$^{-/-}$ mice, LTP was significantly impaired (Figure 4H) and mEPSC amplitudes and frequencies were reduced in *Nptn*$^{\Delta lox/loxPrCreERT}$ mice, indicating presynaptic and postsynaptic changes (Figure 4I). The resulting reduced charge transfer per time and potential seems to be partially compensated by the slower decay and broader half-width of mEPSCs in *Nptn*$^{\Delta lox/loxPrCreERT}$ mice. Strikingly, mIPSCs showed similar changes, i.e., reduced amplitudes and frequencies but delayed decay and increased half-width (Figure 4J). Neuroplastin ablation in mature animals resulted in pronounced differences. For most parameters a similar tendency, although weaker and mostly not statistically significant, was observed in *Nptn*$^{-/-}$ mice. This is most likely explained by interference with developmental processes in *Nptn*$^{-/-}$ mice.

## DISCUSSION

Constitutive *Nptn*$^{-/-}$ mice reveal essential functions of neuroplastins associated with pleiotropic effects on the animal.

**Figure 3.** Inducible reduction of neuroplastin disrupts associative learning and memory with retrograde amnesia. **(A)** Two-way active avoidance learning of wild-type (*Nptn*$^{+/+}$, $n = 13$, black) and *Nptn*$^{-/-}$ ($n = 14$, blue) mice analyzed in a shuttle box with light as the conditioning stimulus. **(B)** Two-way active avoidance learning of *Nptn*$^{lox/lox}$ ($n = 9$, black) or *Nptn*$^{\Delta lox/loxPrCreERT}$ ($n = 11$, blue) mice 8 weeks after tamoxifen induction. **(C)** *Nptn*$^{lox/lox}$ mice with prion CreERT ($n = 7$, blue) or without Cre ($n = 5$, black) were trained for two-way active avoidance to 75% or greater correct responses and then induced with tamoxifen for 10 days, and retested 2 months later. **(D)** *Nptn*$^{lox/lox}$ mice with prion CreERT ($n = 8$, blue) or without Cre ($n = 6$, black) were trained for two-way active avoidance to more than 75% correct responses and then induced with tamoxifen for 10 days, and retrained 2 months later. **(E, F)** *Nptn*$^{lox/lox}$ mice with prion CreERT ($n = 8$, blue) or without Cre ($n = 7$, black) before induction with tamoxifen were subjected to fear conditioning and analyzed for context **(E)** and tone **(F)** memories (before). Then, tamoxifen was administered for 10 days. At 4 and 10 weeks after onset of induction, context and tone memories were analyzed again. **(A–F)** All data are presented as means ± SEM; all $p$ values are derived from Scheffé post hoc test after one- or two-way analysis of variance (*$p < .05$; **$p < .01$; ***$p < .001$). **(G, H)** *Nptn*$^{lox/loxPrCreERT}$ ($n = 7$) and *Nptn*$^{lox/lox}$ ($n = 9$) mice were trained before induction to more than 75% correct responses to the light stimulus in the two-way active avoidance paradigm. Then these mice were induced with tamoxifen for 10 days and retested 8 weeks later under intravenous injection with $^{99m}$Tc-hexmethylpropyleneamineoxime during 10 minutes of ongoing behavior in the shuttle box. Single-photon emission computed tomography/computed tomography images were aligned with a high-resolution magnetic resonance mouse brain data set, and in voxelwise analysis unpaired $t$ tests were made to compare brain tracer distribution. $^{99m}$Tc brain uptake in induced *Nptn*$^{\Delta lox/loxPrCreERT}$ mice compared with *Nptn*$^{lox/lox}$ control mice increased significantly ($p < .0001$) in the right primary visual cortex, anterior olfactory nucleus, lateral septum, left primary somatosensory cortex, left basolateral amygdala, right lateral posterior nucleus of the thalamus/dorsal lateral geniculate nucleus, and right pedunculopontine tegmental areas, and decreased in the left motor cortex, ventromedial hypothalamus, and right ventral hippocampus/amygdalo-hippocampal regions. **(I)** Western blot of membrane fractions (20 μg protein per lane) from brains of wild-type (*Nptn*$^{+/+}$), *Nptn*$^{-/-}$, *Nptn*$^{lox/lox}$ (lox), and *Nptn*$^{\Delta lox/loxPrCreERT}$ (Cre) mice using polyclonal antibodies detecting all forms of plasma membrane $Ca^{2+}$ adenosine triphosphatases. As a control for equal loading, the blot was probed for actin (asterisk). Molecular mass (kDa) of protein standards is indicated on the left.

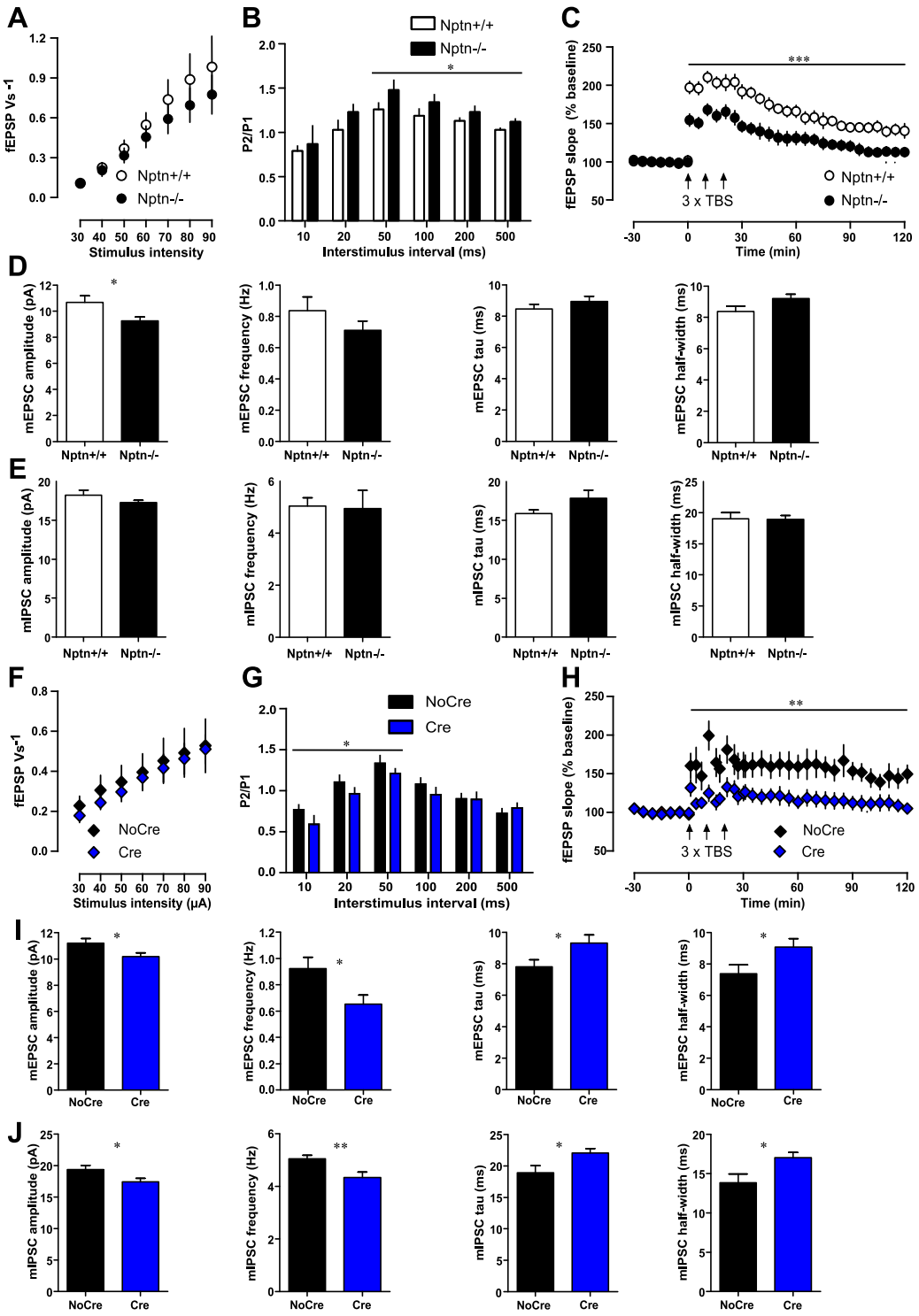
A
fEPSP Vs -1
Nptn+/+
Nptn-/-
Stimulus intensity
B
Nptn+/+
Nptn-/-
P2/P1
Interstimulus interval (ms)
C
fEPSP slope (% baseline)
3 x TBS
Nptn+/+
Nptn-/-
Time (min)
D
mEPSC amplitude (pA)
mEPSC frequency (Hz)
mEPSC tau (ms)
mEPSC half-width (ms)
E
mIPSC amplitude (pA)
mIPSC frequency (Hz)
mIPSC tau (ms)
mIPSC half-width (ms)
F
fEPSP Vs-1
NoCre
Cre
Stimulus intensity (µA)
G
NoCre
Cre
P2/P1
Interstimulus interval (ms)
H
fEPSP slope (% baseline)
3 x TBS
NoCre
Cre
Time (min)
I
mEPSC amplitude (pA)
mEPSC frequency (Hz)
mEPSC tau (ms)
mEPSC half-width (ms)
J
mIPSC amplitude (pA)
mIPSC frequency (Hz)
mIPSC tau (ms)
mIPSC half-width (ms)

Reduced life span, corticosterone elevation, disregulation of the HPA axis, male infertility, less anxious behavior, motivational deficits, altered social interaction, increased despair-like behavior, and learning deficits displayed by *Nptn*$^{-/-}$ mice are potentially related to psychopathologic conditions such as depression, autism, and affective disorders. The role of CAMs in mediating chronic stress-induced signaling, for example, a contribution of neural CAM and L1 in cognitive impairment resulting from stress, has been discussed (36). However, CAM deficiency resulting in chronically elevated corticosterone levels and impaired feedback inhibition of the HPA axis has not been reported. *Nptn*$^{-/-}$ mice display a disturbed balance between excitatory and inhibitory synaptic transmission. Similar imbalances have been implicated in stress-related pathologies including forms of major depression, chronic anxiety, and posttraumatic stress disorder (37–40). Np65 interacts with $GABA_A$ receptor subunit $\alpha_2$ and *Nptn*$^{-/-}$ neurons exhibit impaired inhibitory transmission (9,10). Altered expression of $GABA_A$ receptor subunits has been linked to depression, mood disorders, and schizophrenia (41). Here, we show that diminished neuroplastin expression (about 50% or less) throughout life or after loss in the adult affects PPI of the acoustic startle response, the candidate endophenotype of schizophrenia. Interestingly, a neuroplastin promoter mutation has been associated with schizophrenia (6). In addition, high glucocorticoid levels and/or other components of the stress response increase the risk of developing this disorder (42).

Our previous work confirmed that the differential expression of neuroplastins in the hippocampus could confer circuit specificity (10). Furthermore, neuroplastins exert multiple effects on glutamatergic and GABAergic synapses, resulting in altered electrophysiologic properties of inhibitory and excitatory synapses in *Nptn*$^{-/-}$ and *NPTN*$^{\Delta lox/loxPrCreERT}$, mice as demonstrated by whole-cell recordings of hippocampal CA1 neurons in this study. Inducible neuron-specific loss of neuroplastins, unlike the constitutive deficiency, did not affect the number of glutamatergic synapses, but both result in electrophysiologic deficits. This indicates that neuroplastins directly affect synaptic transmission that is distinguishable from developmental functions. Thus, neuroplastin deficiency may be regarded as a synaptopathy, a term recently coined for diseases and syndromes caused by synaptic malfunctions including some forms of autism and schizophrenia (43).

Neuroplastin deficiency, both constitutive and induced, affects specifically associative learning and memory, e.g., acquisition and retention or retrieval of learned associations, but does not impair all forms of memory. Retrograde amnesia after ablation of neuroplastins was consistently observed specifically for associative memory in the active avoidance and fear conditioning paradigms, but spared other memories. Our data suggest that circuits with highest neuroplastin expression, e.g., involved in nonspatial (associative) memories, are more strongly affected by ablation than are circuits with lower expression, e.g., involved in spatial memories (44), thus altering information processing affecting association-related but not all forms of memory.

Retrograde amnesia of an associative learning task after induced ablation of the neuroplastin gene is a remarkable phenotype not yet reported for any other gene. Although amnesia is a central pathologic trait common to various psychopathologic disorders, the underlying molecular mechanisms are still unknown. The inducible neuroplastin-deficient mouse model clearly singles out one neuronal protein as indispensable for recalling a previously learned associative task. To date, we cannot distinguish retrograde amnesia caused by loss of the memory trace (retention/storage deficit) or the inability to access the memory (retrieval deficit). Hence, brain region or neuron type–specific inactivation of neuroplastin may identify specific loci for associative memories and disentangle molecular mechanisms underlying amnesia. Our data identify neuroplastins as a novel therapeutic target for memory modulation after traumatic experiences and in post-traumatic stress disorder.

## ACKNOWLEDGMENTS AND DISCLOSURES

This work was supported by grants obtained from Deutsche Forschungsgemeinschaft [Grant No. SFB426 (to EDG and DM) and Grant Nos. GRK1167 and SFB854 (to EDG)]. RH-M was partly supported by the German Academic Exchange Service and Deutsche Forschungsgemeinschaft (Grant Nos. GRK1167 and SFB 854). DB, TA, EI, and VS were supported by research grants from Katholieke Universiteit Leuven (Grant Nos. IDO/06/004 and GOA 12/008).

We gratefully acknowledge the technical assistance of Angelika Reichel, Karla Sowa, Daniela Hill, Ines Bodewald, Karla Krautwald, and Andrea Mohrmann; the donation of genomic clones by Kristina Langnäse; and the Karolinska-Institute Stockholm (Johannes Wilbertz) for embryonic stem cell

**Figure 4.** Synaptic transmission and short-term and long-term synaptic plasticity in the hippocampus of *Nptn*$^{-/-}$ and *Nptn*$^{\Delta lox/loxPrCreERT}$ mice. **(A)** Basal synaptic transmission (evoked field excitatory postsynaptic potentials [fEPSP]) did not differ between wild-type (*Nptn*$^{+/+}$, open circles, $n = 6$) and *Nptn*$^{-/-}$ (filled circles, $n = 7$). **(B)** Short-term plasticity as evaluated by paired-pulse facilitation significantly increased at intensities from 50 to 500 ms in *Nptn*$^{-/-}$ mice (filled bars, $n = 6$) compared with wild-type mice (*Nptn*$^{+/+}$, open bars, $n = 7$) (effect of genotype: $F_{1,11} = 5.089$; $p = .045$, repeated-measures analysis of variance [ANOVA]). **(C)** Long-term potentiation induced by triple theta burst stimulation (TBS) resulted in significantly reduced potentiation in *Nptn*$^{-/-}$ mice ($p = .017$, repeated-measures ANOVA). **(D)** *Nptn*$^{-/-}$ mice displayed a significantly reduced miniature excitatory postsynaptic current (mEPSC) amplitude ($n = 10$ per genotype; $p = .029$, $t$ test) and a similar trend in mEPSC frequency. The kinetics of inactivation (decay-time constant tau, half-width) of both mEPSC and miniature inhibitory postsynaptic currents (mIPSCs) were not changed. **(E)** None of the mIPSC parameters was significantly affected. **(F)** Basal synaptic transmission (fEPSPs) was virtually the same in *Nptn*$^{\Delta lox/loxPrCreERT}$ mice (Cre, blue diamonds) and *Nptn*$^{lox/lox}$ control mice (NoCre, black diamonds). **(G)** Paired-pulse facilitation in *Nptn*$^{\Delta lox/loxPrCreERT}$ (Cre, blue bars) was significantly reduced at interpulse intervals between 10 and 100 ms (effect of genotype: $F_{1,24} = 4.383$; $p = .047$, repeated-measures ANOVA). **(H)** Long-term potentiation induced by triple TBS was significantly impaired in *Nptn*$^{\Delta lox/loxPrCreERT}$ mice ($F_{1,13} = 7.084$; $p = .0196$, repeated-measures ANOVA). **(I)** In *Nptn*$^{\Delta lox/loxPrCreERT}$ mice (Cre, blue bars, $n = 9$), mEPSC amplitudes and frequencies were significantly reduced compared with *Nptn*$^{lox/lox}$ (NoCre, black bars, $n = 9$) (amplitude: $p = .0457$; frequency: $p = .0297$, Welch test). The resulting reduced charge transfer per time and potential seemed to be partially compensated by a slower decay and broader half-width of mEPSCs in *Nptn*$^{\Delta lox/loxPrCreERT}$ mice (tau: $p = .0430$; half-width: $p = .0461$, Welch test). **(J)** Strikingly, similar responses were observed for inhibitory responses, i.e., reduced mIPSC amplitudes and frequencies for *Nptn*$^{\Delta lox/loxPrCreERT}$ (Cre, blue bars, $n = 9$) compared with *Nptn*$^{lox/lox}$ (NoCre, black bars, $n = 9$) (amplitude: $p = .0421$; frequency $p = .0128$, Welch test), but delayed decay and increased mIPSC half-width (tau: $p = .0370$; half-width: $p = .0307$, Welch test) were seen.

culture and the generation of mice on a commercial basis. We thank Philip Weber for the donation of prion CreERT mice.

The authors report no biomedical financial interests or potential conflicts of interest.

## ARTICLE INFORMATION

From the Neurogenetics Special Laboratory (SB, DM), Department of Neurochemistry and Molecular Biology (RH-M, EDG), Special Laboratory Electron and Laserscanning Microscopy (RH-M), Research Group Neuropharmacology (FS), Special Laboratory Noninvasive Brain Imaging (FA), Department Systems Physiology (JG), and Special Laboratory for Molecular Biology Techniques (PWB, K-HS), Leibniz Institute for Neurobiology, Magdeburg, Germany; Laboratory of Biological Psychology (VS, TA, El, DB), Katholieke Universiteit Leuven, Leuven, Belgium; Institute for Biochemistry and Cell Biology (KR, K-DF), Otto-von-Guericke University, Magdeburg, Germany; Helmholtz Center for Neurodegenerative Diseases (FA, EDG), Magdeburg, Germany; School of Biological Sciences (PWB), Royal Holloway University of London, Egham, Surrey, United Kingdom; and Center for Behavioral Neurosciences and Medical Faculty (FA, K-HS, EDG), Otto von Guericke University, Magdeburg, Germany

SB, RH-M, and VS contributed equally to this work.

Address correspondence to: Dirk Montag, Privatdozent, Ph.D., Leibniz Institute for Neurobiology, Neurogenetics Special Laboratory, Brenneckestr. 6, Magdeburg 39118, Germany; E-mail: montag@lin-magdeburg.de

Received Sep 27, 2015; revised Mar 12, 2016; accepted Mar 21, 2016.

Supplementary material cited in this article is available online at http://dx.doi.org/10.1016/j.biopsych.2016.03.2107.

## REFERENCES

1. Smalla KH, Matthies H, Langnaese K, Shabir S, Boeckers TM, Wyneken U, *et al*. (2000): The synaptic glycoprotein neuroplastin is involved in long-term potentiation at hippocampal CA1 synapses. Proc Nat Acad Sci USA 97:4327–4332.
2. Dean C, Dresbach T (2006): Neuroligins and neurexins: linking cell adhesion, synapse formation and cognitive function. Trends Neurosci 29:21–29.
3. Dityatev A, Bukalo O, Schachner M (2009): Modulation of synaptic transmission and plasticity by cell adhesion and repulsion molecules. Neuron Glia Biol 4:197–209.
4. Maness PF, Schachner M (2007): Neural recognition molecules of the immunoglobulin superfamily: signaling transducers of axon guidance and neuronal migration. Nat Neurosci 10:19–26; Erratum in: Nat Neurosci 10:263.
5. Desrivières S, Lourdusamy A, Tao C, Toro R, Jia T, Loth E, *et al*. (2014): Single nucleotide polymorphism in the neuroplastin locus associates with cortical thickness and intellectual ability in adolescents. Mol Psychiatry 20:263–274.
6. Saito A, Fujikura-Ouchi Y, Kuramasu A, Shimoda K, Akiyama K, Matsuoka H, *et al*. (2007): Association study of putative promoter polymorphisms in the neuroplastin gene and schizophrenia. Neurosci Lett 411:168–173.
7. Langnaese K, Beesley PW, Gundelfinger ED (1997): Synaptic membrane glycoproteins gp65 and gp55 are new members of the immunoglobulin superfamily. J Biol Chem 272:821–827.
8. Owczarek S, Kiryushko D, Larsen MH, Gajhede M, Sandi C, Berezin V, *et al*. (2010): Neuroplastin-55 binds to and signals through the fibroblast growth factor receptor. FASEB J 24:1139–1150.
9. Sarto-Jackson I, Milenkovic I, Smalla KH, Gundelfinger ED, Kaehne T, Herrera-Molina R, *et al*. (2012): The cell adhesion molecule neuroplastin-65 is a novel interaction partner of gamma-aminobutyric acid type A receptors. J Biol Chem 287:14201–14214.
10. Herrera-Molina R, Sarto-Jackson I, Montenegro-Venegas C, Heine M, Smalla KH, *et al*. (2014): Structure of excitatory synapses and GABAA receptor localization at inhibitory synapses are regulated by neuroplastin-65. J Biol Chem 289:8973–8988.
11. Weber P, Metzger D, Chambon P (2001): Temporally controlled targeted somatic mutagenesis in the mouse brain. Eur J Neurosci 14: 1777–1783.
12. Montag D, Giese KP, Bartsch U, Martini R, Lang Y, Blüthmann H, *et al*. (1994): Mice deficient for the myelin-associated glycoprotein show subtle abnormalities in myelin. Neuron 13:229–246.
13. Montag-Sallaz M, Schachner M, Montag D (2002): Misguided axonal projections, NCAM180 mRNA upregulation, and altered behavior in mice deficient for the Close Homolog of L1 (CHL1). Mol Cell Biol 22: 7967–7981.
14. Montag-Sallaz M, Montag D (2003): Severe cognitive and motor coordination deficits in Tenascin-R-deficient mice. Genes Brain Behav 2:20–31.
15. Montag-Sallaz M, Montag D (2003): Learning-induced arg 3.1 expression in the mouse brain. Learning Memory 10:99–107.
16. Beglopoulos V, Montag-Sallaz M, Rohlmann A, Piechotta K, Ahmad M, Montag D, *et al*. (2005): Neurexophilin 3 is highly localized in cortical and cerebellar regions and is functionally important for sensorimotor gating and motor coordination. Mol Cell Biol 25:7278–7288.
17. Bhattacharya S, Haertel C, Maelicke A, Montag D (2014): Galantamine slows down plaque formation and behavioral decline in the 5XFAD mouse model of Alzheimer's disease. PLoS ONE 9:e89454.
18. Wolfer DP, Mandani R, Valenti P, Lipp HP (2001): Extended analysis of path data from mutant mice using the public domain software Wintrack. Physiol Behav 73:745–753.
19. Schilling S, Zeitschel U, Hoffmann T, Heiser U, Francke M, Kehlen A, *et al*. (2008): Glutaminyl cyclase inhibition attenuates pyroglutamate Aβ and Alzheimer's disease-like pathology *in vivo*. Nat Med 14: 1106–1111.
20. Schmeisser MJ, Ey E, Bockmann J, Wegener S, Stempel V, Kuebler A, *et al*. (2012): Abnormal glutamatergic neurotransmission, hyperactivity and autistic-like behaviours in mice lacking ProSAP1/Shank2. Nature 486:256–260.
21. Can A, Dao DT, Terrillion CE, Piantadosi SC, Bhat S, Gould TD (2012): The tail suspension test. J Vis Exp 59:e3769.
22. Denayer E, Ahmed T, Brems H, Van Woerden G, Borgesius NZ, Callaerts-Vegh Z, *et al*. (2008): Spred1 is required for synaptic plasticity and hippocampus-dependent learning. J Neurosci 28:14443–14449.
23. El-Hassar L, Milh M, Wendling F, Ferrand N, Esclapez M, Bernard C (2007): Cell domain-dependent changes in the glutamatergic and GABAergic drives during epileptogenesis in the rat CA1 region. J Physiol 578:193–211.
24. Torborg CL, Nakashiba T, Tonegawa S, McBain CJ (2010): Control of CA3 output by feedforward inhibition despite developmental changes in the excitation-inhibition balance. J Neurosci 30: 15628–15637.
25. Shao M, Hirsch JC, Peusner KD (2012): Plasticity of spontaneous excitatory and inhibitory synaptic activity in morphologically defined vestibular nuclei neurons during early vestibular compensation. J Neurophysiol 107:29–41.
26. Kolodziej A, Lippert M, Angenstein F, Neubert J, Pethe A, Grosser OS, *et al*. (2014): SPECT-imaging of activity-dependent changes in regional cerebral blood flow induced by electrical and optogenetic self-stimulation in mice. Neuroimage 103:171–180.
27. Ma Y, Hof PR, Grant SC, Blackband SJ, Bennett R, Slatest L, *et al*. (2005): A three-dimensional digital atlas database of the adult C57BL/6 J mouse brain by magnetic resonance microscopy. Neuroscience 135:1203–1215.
28. Ma Y, Smith D, Hof PR, Foerster B, Hamilton S, Blackband SJ, *et al*. (2008): In vivo 3D digital atlas database of the adult C57BL/6 J mouse brain by magnetic resonance microscopy. Front Neuroanat 2008 Apr 17; 2:1. http://dx.doi.org/10.3389/neuro.05.001.2008. eCollection 2008.
29. Endepols H, Sommer S, Backes H, Wiedermann D, Graf R, Hauber W (2010): Effort-based decision making in the rat: an [18F]fluorodeoxyglucose micro positron emission tomography study. J Neurosci 30: 9708–9714.
30. Thanos PK, Robison L, Nestler EJ, Kim R, Michaelides M, Lobo MK (2013): Mapping brain metabolic connectivity in awake rats with μPET and optogenetic stimulation. J Neurosci 33:6343–6349.

31. Wyckhuys T, Staelens S, Van Nieuwenhuyse B, Deleye S, Hallez H, Vonck K, *et al*. (2010): Hippocampal deep brain stimulation induces decreased rCBF in the hippocampal formation of the rat. Neuroimage 52:55–61.
32. Nagy A, Moens C, Ivanyi E, Pawling J, Gertsenstein M, Hadjantonakis AK, *et al*. (1998): Dissecting the role of N-myc in development using a single targeting vector to generate a series of alleles. Curr Biol 8: 661–664.
33. Frodl T, O'Keane V (2013): How does the brain deal with cumulative stress? A review with focus on developmental stress, HPA axis function and hippocampal structure in humans. Neurobiol Dis 52: 24–37.
34. Augustine GJ, Santamaria F, Tanaka K (2003): Local calcium signaling in neurons. Neuron 40:331–346.
35. Simons SB, Escobedob Y, Yasudab R, Dudeka SM (2009): Regional differences in hippocampal calcium handling provide a cellular mechanism for limiting plasticity. Proc Natl Acad Sci USA 106: 14080–14084.
36. Sandi C (2004): Stress, cognitive impairment and cell adhesion molecules. Nat Rev Neurosci 5:917–930.
37. Shabel SJ, Proulx CD, Piriz J, Malinow R (2014): Mood regulation: GABA/glutamate co-release controls habenula output and is modified by antidepressant treatment. Science 345:1494–1498.
38. Chrousos GP (2000): The role of stress and the hypothalamic-pituitary-adrenal axis in the pathogenesis of the metabolic syndrome: neuro-endocrine and target tissue-related causes. Int J Obes Relat Metab Disord 24(suppl 2):S50–S55.
39. Elenkov IJ, Chrousos GP (2002): Stress hormones, proinflammatory and antiinflammatory cytokines, and autoimmunity. Ann NY Acad Sci 966:290–303.
40. Gao SF, Bao AM (2011): Corticotropin-releasing hormone, glutamate, and γ-aminobutyric acid in depression. Neuroscientist 17: 124–144.
41. Fatemi SH, Folsom TD, Rooney RJ, Thuras PD (2013): Expression of GABAA α2-, β1- and ε-receptors are altered significantly in the lateral cerebellum of subjects with schizophrenia, major depression and bipolar disorder. Transl Psych 3:e303. http://dx.doi.org/10.1038/tp.2013.64.
42. Koenig JI, Kirkpatrick B, Lee P (2002): Glucocorticoid hormones and early brain development in schizophrenia. Neuropsychopharmacology 27:309–318.
43. Grant SG (2012): Synaptopathies: diseases of the synaptome. Curr Opin Neurobiol 22:522–529.
44. Nakamura NH, Flasbeck V, Maingret N, Kitsukawa T, Sauvage MM (2013): Proximodistal segregation of nonspatial information in CA3: preferential recruitment of a proximal CA3-distal CA1 network in nonspatial recognition memory. J Neurosci 33:11506–11514.